Molecular Plant Pathology

MOLECULAR PLANT PATHOLOGY (2016) **17**(1), 3–15 DOI: 10.1111/mpp.12257

Activation of senescence-associated *Dark-inducible* (*DIN*) genes during infection contributes to enhanced susceptibility to plant viruses

LOURDES FERNÁNDEZ-CALVINO[1,†], IRENE GUZMÁN-BENITO[1,2], FRANCISCO J. DEL TORO[1], LIVIA DONAIRE[1], ANA B. CASTRO-SANZ[1,†], VIRGINIA RUÍZ-FERRER[1] AND CÉSAR LLAVE[1,*]

[1]*Department of Environmental Biology, Centro de Investigaciones Biológicas, CSIC, Ramiro de Maeztu 9, 28040 Madrid, Spain*
[2]*Doctorado en Biotecnología y Recursos Genéticos de Plantas y Microorganismos Asociados, ETSI Agronómica, Alimentaria y de Biosistemas, Universidad Politécnica de Madrid, 28040-Madrid, Spain*

SUMMARY

Virus infections in plants cause changes in host gene expression that are common to other environmental stresses. In this work, we found extensive overlap in the transcriptional responses between *Arabidopsis thaliana* plants infected with *Tobacco rattle virus* (TRV) and plants undergoing senescence. This is exemplified by the up-regulation during infection of several senescence-associated *Dark-inducible* (*DIN*) genes, including At*DIN1* (*Senescence 1*, *SEN1*), At*DIN6* (*Asparagine synthetase 1*, At*ASN1*) and At*DIN11*. *DIN1*, *DIN6* and *DIN11* homologues were also activated in *Nicotiana benthamiana* in response to TRV and *Potato virus X* (PVX) infection. Reduced TRV levels in RNA interference (RNAi) lines targeting At*DIN11* indicate that *DIN11* is an important modulator of susceptibility to TRV in Arabidopsis. Furthermore, low accumulation of TRV in Arabidopsis protoplasts from RNAi lines suggests that At*DIN11* supports virus multiplication in this species. The effect of *DIN6* on virus accumulation was negligible in Arabidopsis, perhaps as a result of gene or functional redundancy. However, TRV-induced silencing of Nb*ASN*, the *DIN6* homologue in *N. benthamiana*, compromises TRV and PVX accumulation in systemically infected leaves. Interestingly, Nb*ASN* inactivation correlates with the appearance of morphological defects in infected leaves. We found that *DIN6* and *DIN11* regulate virus multiplication in a step prior to the activation of plant defence responses. We hypothesize on the possible roles of *DIN6* and *DIN11* during virus infection.

Keywords: *Arabidopsis thaliana*, *Dark-inducible* (*DIN*) genes, *Nicotiana benthamiana*, plant viruses, *Potato virus X*, senescence-associated genes, *Tobacco rattle virus*.

INTRODUCTION

Plants respond to pathogen infection by reprogramming host gene expression, which includes, among others, the induction of a suite of defence- and pathogenesis-related genes (van Loon *et al*., 2006; Wise *et al*., 2007). The expression of defence-related genes is also triggered during senescence, a process of programmed cell death that occurs in response to developmental, physical, physiological and hormonal cues (Buchanan-Wollaston *et al*., 2003; Gepstein *et al*., 2003; Lim and Nam, 2005; Quirino *et al*., 2000). Interestingly, senescence-associated genes are activated during pathogen attack, which is suggestive of common events or signalling pathways in the control of gene expression in these two overlapping processes (Lin and Wu, 2004; Quirino *et al*., 1999). Some senescence-enhanced genes are detected during the hypersensitive response against incompatible bacteria and fungi and against virulent or avirulent pathogens that cause necrosis (Pontier *et al*., 1999; Schenk *et al*., 2005). This observation could lead to the misleading assumption that cell death is the necessary point of convergence between defence and senescence. However, senescence-related genes are also expressed at elevated levels during compatible interactions between plants and viruses (Espinoza *et al*., 2007; Whitham *et al*., 2003). Hence, the execution of the cell death programme seems to be uncoupled from the initial regulation of senescence. Cellular stress is the most likely factor explaining why senescence-related genes are activated during pathogen-activated responses. Indeed, many stress-inducible genes are up-regulated during senescence, which implies that cells undergoing senescence are subjected to stress conditions (Gepstein *et al*., 2003; Weaver *et al*., 1998). In addition, stresses caused by drought, darkness, sugar starvation, wounding or leaf detachment initiate the senescence programme (Lin and Wu, 2004; Weaver *et al*., 1998). The extent and significance of this overlap and the precise roles of pathogen- and senescence-responsive pathways remain largely unknown.

The production of reactive oxygen species (ROS) is a unifying response to multiple stresses and, consequently, has been proposed as a common signal controlling gene expression in stressed plants (Love *et al*., 2005; Quirino *et al*., 2000; Torres and Dangl, 2005). Senescence and pathogen infection are both accompanied by a certain degree of cellular damage caused by oxidative stress and, accordingly, ROS detoxification genes are stimulated in both types of process (Buchanan-Wollaston *et al*., 2003; Espinoza *et al*., 2007; Schippers *et al*., 2008; Whitham

**Correspondence*: Email: cesarllave@cib.csic.es
†*Present address*: Centro de Biotecnología y Genómica de Plantas, Campus Montegancedo, Pozuelo de Alarcón, 28223 Madrid, Spain.

[Corrections added on 13 June 2019, after first online publication: A second affiliation has been added to the second author in this version].

et al., 2003). For instance, glutamate dehydrogenase (GDH), which is activated by both senescence and viral or bacterial infections, is highly expressed under oxidative stress (Pageau *et al*., 2006). Chemical signal compounds, such as salicylic acid (SA) and methyl jasmonate (MeJA), which have defensive and senescence-promoting functions, regulate the expression of certain senescence- and pathogen-associated genes (Schenk *et al*., 2005). Changes in the source-to-sink balance, normally associated with pathogen invasions, are also pivotal in regulating leaf senescence (Herbers *et al*., 2000; Masclaux *et al*., 2000; Shalitin and Wolf, 2000).

In this study, we have identified a set of genes, collectively named *Dark-inducible* (*DIN*), that actively respond to *Tobacco rattle virus* (TRV) infection in *Arabidopsis thaliana*. *DIN* genes are induced in dark-adapted and senescing leaves (Fujiki *et al*., 2001, 2005; Lin and Wu, 2004; Quirino *et al*., 2000), and inspection of Arabidopsis microarray data using Genevestigator indicates that *DIN* genes also respond to biotic stimuli. This finding suggests that *DIN* genes could participate in cellular events that are common to both senescence and pathogen invasion (Zimmermann *et al*., 2004). However, although some *DIN* genes, such as *DIN1*, *DIN6* and *DIN11*, have been used previously as markers to characterize senescence-associated responses, their regulation and function during compatible interactions between viruses and host plants are largely unknown (Lam *et al*., 1994; Oh *et al*., 1996; Schenk *et al*., 2005). Here, we show that *DIN6*- and *DIN11*-encoding enzymatic activities may play critical roles in the modulation of plant susceptibility to virus infection.

RESULTS

Gene expression profiling reveals significant similarities between TRV infection and senescence in Arabidopsis

To discriminate the group of genes whose expression was similarly regulated in response to TRV infection and senescence, we compared microarray data of the Arabidopsis response to TRV with gene expression profiling data during developmental or dark-induced leaf senescence (Buchanan-Wollaston *et al*., 2005; Fernandez-Calvino *et al*., 2014; Lin and Wu, 2004). Global transcriptomic changes in TRV-infected Arabidopsis plants were documented at 8 days after inoculation (dai), when TRV has been shown to exhibit the highest peak of genomic RNA accumulation (Fernandez-Calvino *et al*., 2014). TRV-responsive genes (Bonferroni-corrected $P < 0.01$) were compared with the list of genes described above. We found a group of 68 genes that responded similarly to virus infection, dark-induced senescence and age-mediated (natural) senescence [Table S1 (Supporting Information) and Fig. 1A]. Interestingly, 61% of the TRV-responsive genes (724 genes) were altered in the same direction (either induced or repressed) when senescence was artificially induced by darkness or carbon starvation, and 8% (97 genes) were shared between TRV infection and developmental leaf senescence. In both cases, the number of common genes in the intersection between TRV infection and dark-induced senescence or developmental senescence was higher than that expected in a random distribution ($P < 0.0001$), indicating significant commonalities in their transcriptional responses (Fig. 1A). Using an independent set of plants, and consistent with microarray data, quantitative reverse transcription-polymerase chain reaction (qRT-PCR) revealed increased transcript levels of the stress-inducible *Senescence-associated gene 13* (At*SAG13*, At2g29350) at 8 dai (Fig. 1B) (Gan and Amasino, 1997; Weaver *et al*., 1998).

Despite the extensive degree of overlap in the transcriptomic responses of TRV-infected leaves and leaves undergoing senescence (Fig. 1A), TRV infection in Arabidopsis apparently proceeds in the absence of macroscopic alterations that could be diagnostic of accelerated induction of leaf senescence (Lin *et al*., 2009; Quirino *et al*., 2000). To accurately determine the effect of virus infection on plant growth and development, we measured a series of morphological traits in vegetative and reproductive organs in mock-inoculated and TRV-infected plants at 16 and 29 dai. None of the growth-related traits tested differed significantly between healthy and TRV-infected plants (Figs 1C and S1, see Supporting Information). Likewise, equivalent numbers of viable seeds and seed weight were produced by infected and mock-inoculated plants (Fig. 1C). Chlorophyll breakdown during chloroplast disassembly is a typical visible manifestation of senescence (Quirino *et al*., 2000). However, chlorophyll content remained at comparable levels in mock-inoculated and TRV-infected leaves at 16 and 29 dai (Figs 1D and S1). We also determined electrolyte leakage to assess whether virus infection caused membrane damage. Our results indicated a similar percentage of electrolyte leakage in leaves inoculated with TRV and in upper non-inoculated TRV-infected leaves with respect to the corresponding non-infected leaves, even at later time points after infection (Figs 1E and S1). Collectively, the overlap in the transcriptional responses between TRV infection and both types of senescence suggests a significant interaction between these two stress-related processes, which, however, did not reflect a premature ongoing senescence-like phenotype.

TRV stimulates the expression of *DIN* genes in Arabidopsis

Among the genes that exhibited similar responsiveness to TRV in different Arabidopsis organs (F. J. del Toro and C. Llave, unpublished data), we identified several senescence-associated genes catalogued as *DIN* genes. The gene expression data and predicted functions of Arabidopsis *DIN* genes deduced from their amino acid sequences are shown in Table 1. To validate microarray-based

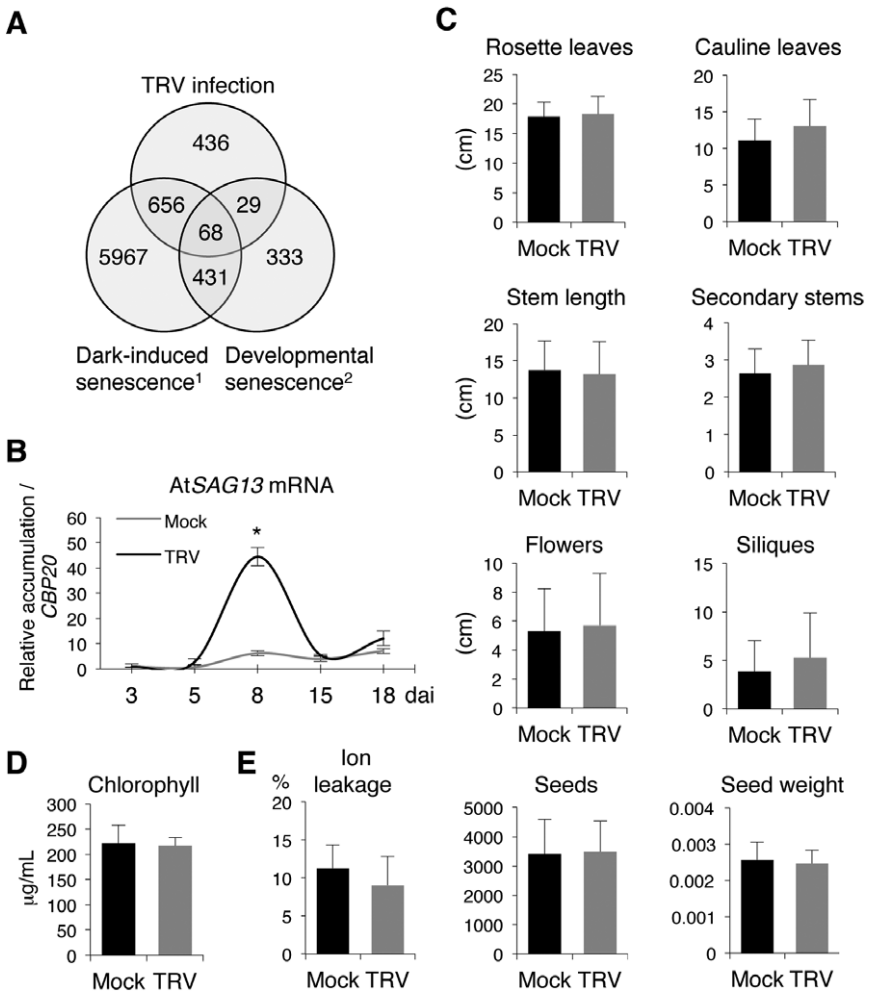

Fig. 1 Analysis of senescence-associated traits during *Tobacco rattle virus* (TRV) infection in Arabidopsis. (A) Venn diagram to illustrate the number of specific and common misregulated genes in dark-induced senescence, natural senescence and TRV infection in Arabidopsis. Genes showing significant TRV responsiveness were compared with Affymetrix expression data from the two types of senescence: 1, Lin and Wu (2004); 2, Buchanan-Wollaston *et al*. (2005). The numbers of genes within the intersections are higher than those expected by chance. To test whether the significance of matches was higher than explained by random sampling, we assumed a Poisson distribution from a mean value calculated as $\mu = G1 \times (G2/Gt)$, as any gene in G1 has a G2/Gt possibility of belonging to G2, where G1 and G2 are the subsets of genes to be compared and Gt is the total number of genes represented in the microarray. (B) Time-course expression of the stress senescence marker At*SAG13* in TRV-infected plants examined by quantitative reverse transcription-polymerase chain reaction (qRT-PCR). The means of three measurements ± standard deviation (SD) are shown. Values are relative to those in mock-inoculated plants at 3 days after inoculation (dai) which were arbitrarily assigned a value of unity after normalization to the At*CBP20* internal control. Asterisks indicate significant difference from the mock-inoculated control ($P < 0.001$, Duncan's multiple range test). (C) Effect of TRV infection on the number of rosette and cauline leaves, secondary stems, inflorescences and siliques, and stem length (cm) at 16 dai. Total seed number and weight (g) were used to quantify progeny production. (D) Total chlorophyll content in Arabidopsis leaves at 16 dai. (E) Activation of cell death measured by leakage of ions in mock-inoculated and TRV-infected plants at 16 dai. The means and SD of three independent replicates are shown.

expression of *DIN* genes in TRV-infected Arabidopsis, we conducted qRT-PCR on the same pooled RNA extracts as used for microarray hybridization, as well as on an independent set of samples (not used for microarrays), to confirm reproducibility in their expression patterns. According to this analysis, At*DIN1* (also *Senescence 1*, At*SEN1*) and *Asparagine synthetase 1* (At*ASN1*), the Arabidopsis homologue of *DIN6* (herein referred to as *DIN6* for simplicity), transcripts were significantly more abundant in TRV-infected tissue than in the non-infected control in the two sets of samples collected from leaves, inflorescences and roots (Fig. 2). These results corroborated the microarray-based prediction that At*DIN1* and At*DIN6* were strongly and widely activated by TRV. qRT-PCR demonstrated that At*DIN11*, which was not represented in the CATMA (Complete Arabidopsis Transcriptome MicroArray) used, was induced by TRV in all three tissues analysed using independent RNA preparations (Fig. 2). In this study, we focus on

Table 1 Microarray-based expression changes in *Dark-inducible* (*DIN*) genes in three Arabidopsis organs.

Gene	AGI	Protein description	Fold change†		
			Leaves	Inflorescences	Roots
DIN1	At4g35770	Senescence-associated gene 1 (SEN1)	**7.31*****	**4.75*****	**3.58*****
DIN2	At3g60140	β-Glucosidase 30, Senescence-associated gene 2 (SEN2)	1.04	−0.98	1.04
DIN3	At3g06850	Dihydrolipoamide branched chain acyltransferase (BCE2)	1.06	**1.44***	**1.86*****
DIN4	At3g13450	Branched chain α-keto acid dehydrogenase E1 β	**1.91****	**2.65*****	**1.5****
DIN6	At3g47340	Glutamine-dependent asparagine synthetase 1 (ASN1)	**2.05*****	**3.01*****	**1.89*****
DIN9	At1g67070	Phosphomannose isomerase 2 (PMI2)	−0.96	−0.97	1.00
DIN10	At5g20250	Raffinose synthase 6 (RS6)	−0.82	**4.5*****	**1.94*****
DIN11	At3g49620	2-Oxoacid-dependent dioxygenase	ND‡	ND	ND

†Bold numbers indicate significant differences in gene expression between mock-inoculated and *Tobacco rattle virus* (TRV)-infected plants. Differences from control values were significant at $P < 1 \times 10^{-12}$ (***), $P < 0.01$ (**) or $P < 0.05$ (*) (Bonferroni-corrected method).
‡ND, not detected.

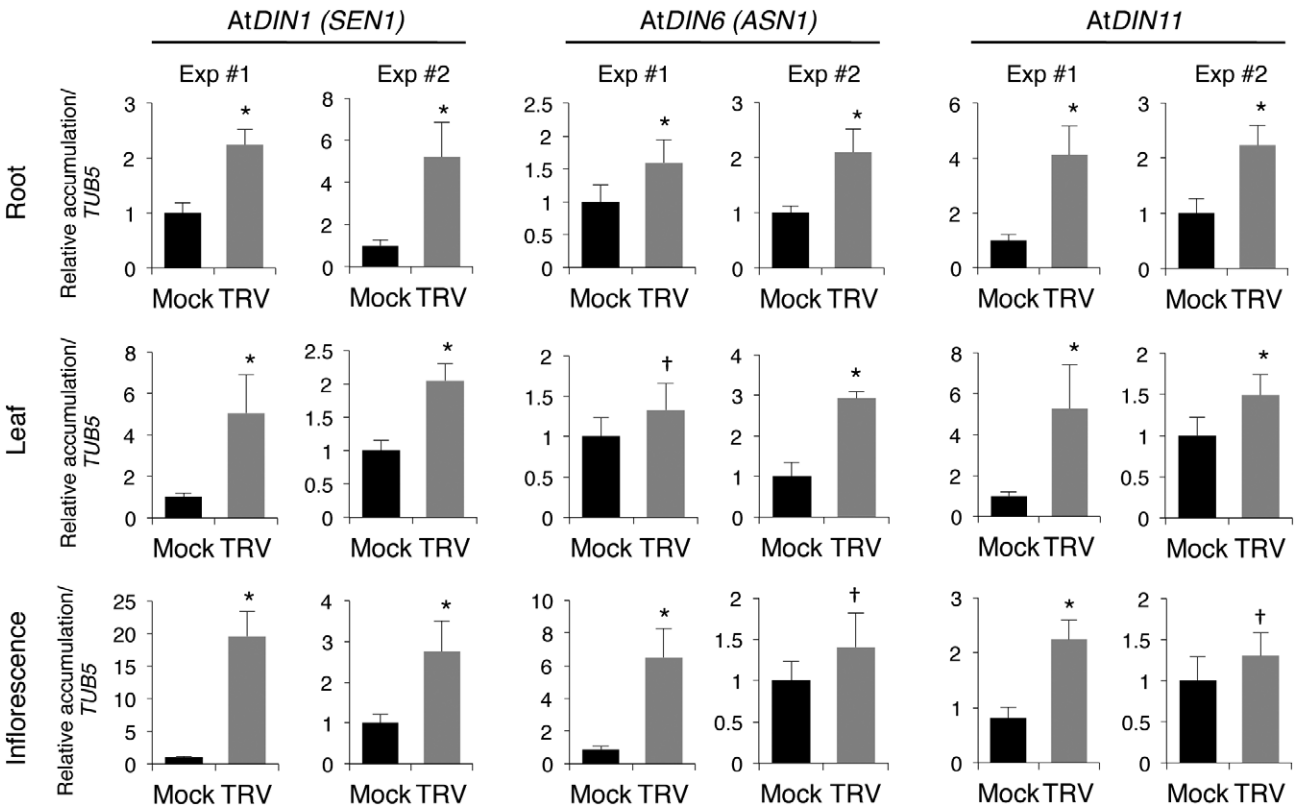

Fig. 2 Expression of *Dark-inducible* (*DIN*) genes in response to *Tobacco rattle virus* (TRV) infection in Arabidopsis. Transcript levels of At*DIN1* (*Senescence 1*, *SEN1*), At*DIN6* (*Asparagine synthetase 1*, *ASN1*) and At*DIN11* were examined by quantitative reverse transcription-polymerase chain reaction (qRT-PCR) in two independent experiments (Exp #1 and Exp #2). The means of three measurements ± standard deviation (SD) are shown. Values are given relative to those in mock-inoculated plants that were arbitrarily assigned a value of unity after At*TUB5* normalization. Samples were collected from roots and non-inoculated rosette leaves at 8 days after inoculation (dai) and inflorescences at 12 dai. Differences from control values were significant at $P < 0.001$ (*) or $P < 0.05$ (†) (Duncan's multiple range test).

At*DIN1*, At*DIN6* and At*DIN11*, given that these three genes were significantly up-regulated and exhibited broad responsiveness throughout the plant (Table 1).

Microarray data indicated the deregulation of other dark-responding genes in the presence of TRV, although changes in their expression patterns were not very reproducible between organs or batches of plants. In general, At*DIN3* and At*DIN10* were activated by TRV in both inflorescences and roots, and their mRNA accumulation patterns were confirmed by qRT-PCR in independent RNA samples (Fig. S2, see Supporting Information). Although

microarray data did not reflect differential changes in At*DIN3* or At*DIN10* expression in leaves, qRT-PCR showed that At*DIN10* mRNA levels were substantially reduced using independent samples from infected relative to non-infected leaves, whereas At*DIN3* was either repressed or unaffected by TRV (Fig. S2). We found that At*DIN2* transcripts, which did not exhibit TRV responsiveness on the basis of microarray-based expression profiling, were significantly more abundant in both sets of samples from roots and leaves when assessed using qRT-PCR (Fig. S2). Finally, our gene expression tests indicated that At*DIN9* was consistently up-regulated in inflorescences on TRV challenge, whereas transcript accumulation varied when roots and leaves were analysed (Fig. S2).

At*DIN11* enhances susceptibility to TRV in Arabidopsis

To assess the contribution of *DIN1*, *DIN6* and *DIN11* to TRV infection, we used Arabidopsis knockout lines of these genes to monitor virus accumulation. qRT-PCR revealed that TRV accumulated in single *din1* or *din6* mutants to the same levels as in the wild-type background, suggesting that neither At*DIN1* nor At*DIN6* was critical for viral susceptibility in Arabidopsis (Fig. 3A,B). To test At*DIN11* contribution to TRV infection, we obtained transgenic Arabidopsis plants harbouring a hairpin dsRNA-based RNA interference (RNAi) construct targeted against the At*DIN11* gene. Total RNA from systemically infected rosette leaves of two independent homozygous T3 Arabidopsis lines (L10 and L21) infected with TRV was subjected to qRT-PCR experiments. In these plants, At*DIN11* transcript levels were reduced by more than 80% compared with wild-type controls, demonstrating the effective silencing of the targeted gene (Fig. 3C). Silencing of At*DIN11* in both L10 and L21 RNAi lines correlated with a significant two-fold reduction in TRV accumulation compared with wild-type plants at 5 and 8 dai (Fig. 3C). Interestingly, TRV levels showed large differences between independent replicates and genetic backgrounds at 16 dai (data not shown), suggesting that the influence of *DIN11* on TRV accumulation could be restricted to the early time points of infection during which virus proliferation is particularly dynamic. To test this hypothesis, we isolated protoplasts from Arabidopsis rosette leaves and subjected them to transfection with the infectious pTRV1 vector. qRT-PCR of total RNA extracted at 24 h post-transfection demonstrated that viral replication was severely compromised in both L10 and L21 lines (Fig. 3D). This result was highly reproducible, confirming that a functional *DIN11* was required to allow virus multiplication. No major visible morphological differences were observed between knockout or RNAi lines and wild-type plants (data not shown).

TRV and *Potato virus X* (PVX) promote the expression of Nb*NRIP1*, Nb*ASN* and Nb*DIN11* in infected *Nicotiana benthamiana*

We were interested in determining whether TRV-mediated induction of *DIN1*, *DIN6* or *DIN11* was unique to Arabidopsis or whether

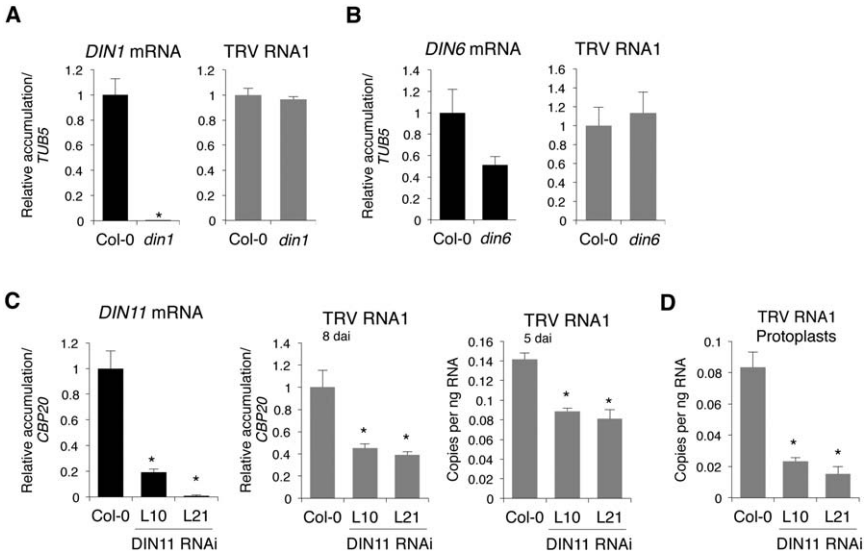

Fig. 3 Effect of *Dark-inducible* (*DIN*) genes on *Tobacco rattle virus* (TRV) susceptibility in Arabidopsis. Transcript accumulation, determined by quantitative reverse transcription-polymerase chain reaction (qRT-PCR), is given relative to that in wild-type plants that were assigned a value of unity after normalization. The absolute quantification of TRV RNA1 is given as the number of viral copies per nanogram of total RNA. Means of three measurements ± standard deviation (SD) are shown. Asterisks indicate statistical significance versus the wild-type control ($P < 0.001$, Duncan's multiple range test). (A, B) Analysis of At*DIN1* (A) and At*DIN6* (B) expression and accumulation of TRV RNA1 in TRV-infected Arabidopsis leaves of *din*1 (A) and *din6* (B) mutants at 8 days after inoculation (dai). (C) Analysis of At*DIN11* expression and accumulation of TRV genomic RNA1 in infected leaves of Arabidopsis *DIN11* RNAi lines (L10 and L21) at 5 dai (absolute quantification) and 8 dai (relative quantitation). (D) Accumulation of TRV RNA1 in Arabidopsis protoplasts from L10 and L21 lines 24 h after transfection.

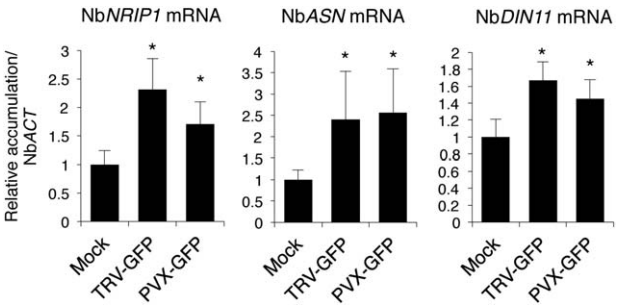

Fig. 4 Expression of *Dark-inducible* (*DIN*) homologues in *Nicotiana benthamiana* in response to *Tobacco rattle virus* (TRV) and *Potato virus X* (PVX). Quantitative reverse transcription-polymerase chain reaction (qRT-PCR) analysis of Nb*NRIP1* (*N receptor-interacting protein 1*), Nb*ASN* (*Asparagine synthetase 1*) and Nb*DIN11* expression in upper non-inoculated leaves of plants infected with TRV-GFP or PVX-GFP. Accumulation levels are referenced to the mock-inoculated controls that were arbitrarily assigned a value of unity after normalization to the Nb*ACT* internal control. The means of three measurements ± standard deviation (SD) are shown. Asterisks indicate statistical significance versus the mock-inoculated control ($P < 0.001$, Duncan's multiple range test). GFP, green fluorescent protein.

these genes responded to TRV infection in other susceptible hosts. To test this possibility, we first conducted a BLAST search using Arabidopsis *DIN* genes as queries to find putative *DIN* homologue genes in the *N. benthamiana* expressed sequence tag (EST) database. Our homology-based search identified chloroplastic *N receptor-interacting protein 1* (Nb*NRIP1*) (EU332891) and Nb*ASN* (GQ354808) as genes homologous to Arabidopsis At*DIN1* (At4g35770) and At*DIN6* (At3g47340), respectively. We failed to identify sequences with extensive sequence similarity to Arabidopsis At*DIN11* (At3g49620) through database mining in *N. benthamiana* (*N. benthamiana* transcriptome v5 primary transcripts database; http://sydney.edu.au/science/molecular_bioscience/benthamiana/, University of Sydney, Sydney, Australia). However, we were able to amplify an *N. benthamiana* cDNA product using PCR primers designed from highly conserved sequence domains of *Solanum tuberosum* (DQ200393.1) and *S. lycopersicum* ESTs (AK321665.1), that each showed a sequence identity of approximately 67% at the nucleotide level with At*DIN11*, suggesting that a *DIN11* homologue exists in the *N. benthamiana* genome.

We then inoculated *N. benthamiana* plants with TRV, and mRNA accumulation was registered for each *DIN* gene in the upper non-inoculated leaves. qRT-PCR assays indicated that Nb*NRIP1*, Nb*ASN* and putative Nb*DIN11* transcripts accumulated to significantly higher levels in *N. benthamiana* in the presence of TRV relative to mock-inoculated plants (Fig. 4). These results were fully reproducible in independent experiments and demonstrated that the *DIN* homologues Nb*NRIP1*, Nb*ASN* and Nb*DIN11* are induced by TRV in different host species.

We next wanted to test whether these three *DIN* genes were activated in *N. benthamiana* in response to other RNA viruses. To test this, we agroinjected *N. benthamiana* leaves with a PVX-green fluorescent protein (PVX-GFP) clone, and the upper non-inoculated leaves were analysed for transcript accumulation. qRT-PCR revealed that Nb*NRIP1*, Nb*ASN* and Nb*DIN11* endogenous transcripts were increased significantly by more than 50% in PVX-infected plants relative to mock plants agroinfiltrated with an empty vector (Fig. 4). These results demonstrate that *DIN1*, *DIN6* and *DIN11* are potential targets of regulation during infections by different viruses in different hosts.

Suppression of Nb*ASN* compromises susceptibility to TRV and PVX in *N. benthamiana*

To investigate the influence of Nb*NRIP1*, Nb*ASN* and Nb*DIN11* genes on TRV susceptibility in *N. benthamiana*, we tested whether the inactivation of the endogenous *DIN* genes affected the multiplication and spread of TRV in this species. We took advantage of our TRV infectious clone as a vector for virus-induced gene silencing (VIGS) to knock down the expression of the target *DIN* genes. A mixture of *Agrobacterium* cultures containing TRV1 and a recombinant TRV2 clone that carried a fragment of the target gene was co-infiltrated on *N. benthamiana* leaves as described previously (Fig. 5A) (Liu *et al*., 2002). Expression of the targeted *DIN* transcripts was monitored alongside TRV accumulation using qRT-PCR in the upper non-infiltrated leaves 17 days after agroinjection. A TRV-GFP clone that carried the GFP coding sequence gene was used as a control. To accurately amplify endogenous Nb*NRIP1*, Nb*ASN* and Nb*DIN11* transcripts, qRT-PCR primers were designed from regions located outside of those cloned into the corresponding TRV derivatives used for silencing.

When a recombinant TRV-NbNRIP1 infectious clone that harboured a fragment of the Nb*NRIP1* gene was introduced into *N. benthamiana* plants, we observed a five-fold decrease in endogenous Nb*NRIP1* transcript levels in the upper leaves relative to plants infected with a TRV-GFP construct (Fig. 5B). Similarly, infection of *N. benthamiana* plants with the recombinant TRV-NbDIN11 clone that carried a fragment of the potato homologue of *DIN11* resulted in a two- to five-fold reduction in the relative Nb*DIN11* transcript levels compared with control plants (Fig. 5C and data not shown). These results demonstrate the robustness of silencing of the target genes and validate our experimental approach. qRT-PCR also revealed that TRV-genomic RNA accumulated in these silenced leaves to the same high levels as those in plants infected with TRV-GFP, suggesting that silencing of Nb*NRIP1* or Nb*DIN11* was not sufficient to alter virus accumulation (Fig. 5B,C).

Agrobacterium-mediated infiltration of TRV-NbASN, which contained a fragment of the *DIN6* Arabidopsis homologue, resulted in approximately 90% inhibition of Nb*ASN* expression in systemi-

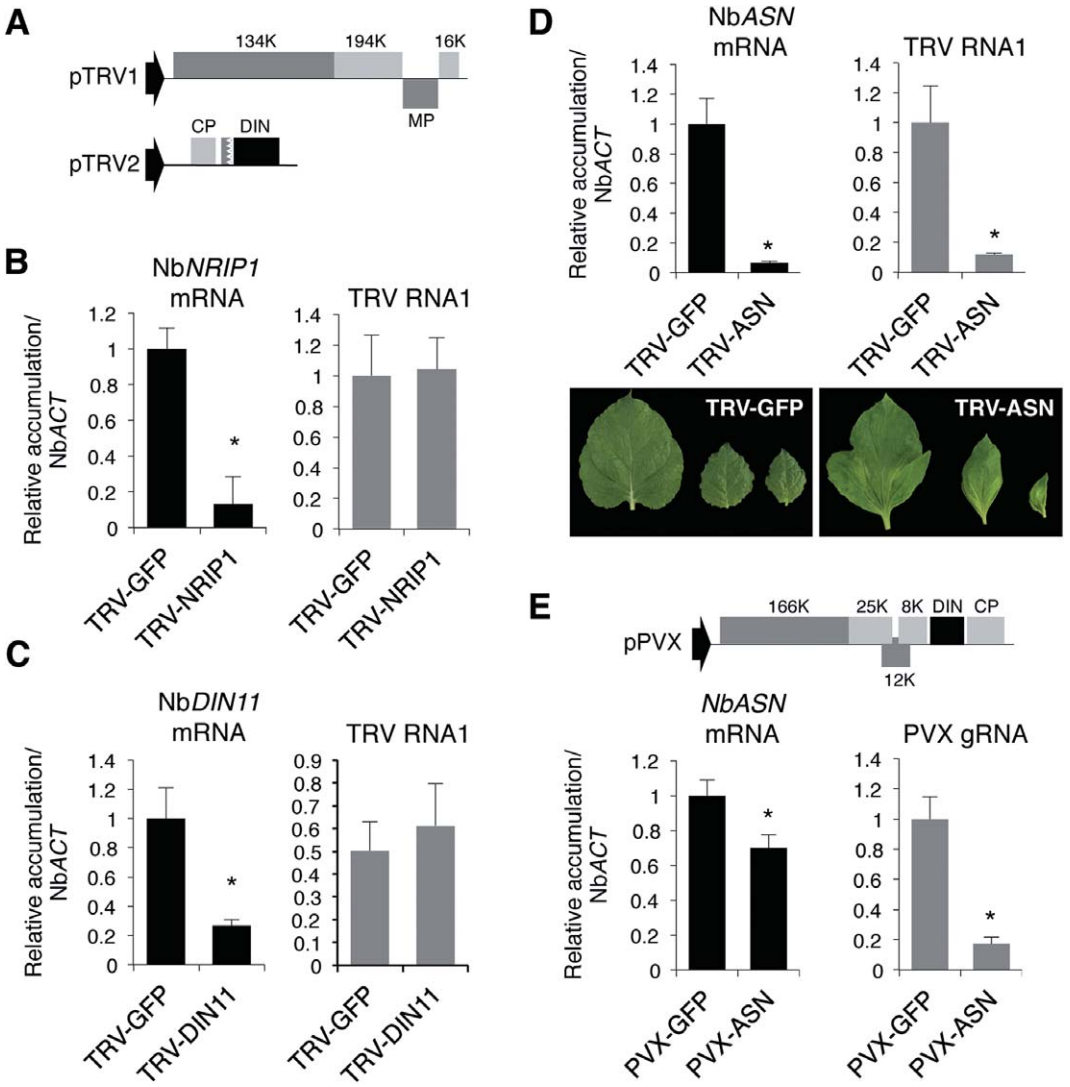

Fig. 5 Effect of silencing of *Dark-inducible* (*DIN*) genes on virus accumulation and symptom expression in *Nicotiana benthamiana* plants. Expression values, determined by quantitative reverse transcription-polymerase chain reaction (qRT-PCR), are relative to those in plants infected with *Tobacco rattle virus*-green fluorescent protein (TRV-GFP) or *Potato virus X*-green fluorescent protein (PVX-GFP) that were assigned a value of unity after Nb*ACT* normalization. The means of three measurements ± standard deviation (SD) are shown. Asterisks indicate significant difference from the TRV-GFP/PVX-GFP control ($P < 0.001$, Duncan's multiple range test). (A) Genome organization of the TRV-based virus-induced gene silencing (VIGS) vectors used for silencing of endogenous *N. benthamiana DIN* homologues. (B, C) Analysis of *NbNRIP1* (B) and *NbDIN11* (C) expression and TRV RNA1 accumulation in upper leaves of plants infected with TRV-NbNRIP1 (B) or TRV-NbDIN11 (C). (D) Analysis of *NbASN* (*Asparagine synthetase 1*) expression and accumulation of TRV RNA1 in upper leaves infected with TRV-NbASN. Symptoms associated with silencing of *NbASN* in TRV-infected leaves are shown relative to the asymptomatic infection caused by TRV-GFP. (E) Analysis of Nb*ASN* expression and PVX genomic RNA accumulation in upper leaves infected with PVX-NbASN and PVX-GFP. The genome organization of the PVX derivative used to silence *NbASN* is shown.

cally infected leaves relative to plants infected with the TRV-GFP control (Fig. 5D). Strikingly, suppression of Nb*ASN* expression in plants infected with TRV-NbASN was reproducibly accompanied by the appearance of dispersed chlorotic areas and leaf deformation that became conspicuous in the youngest apical leaves at approximately 15 dai (Fig. 5D). In addition, Nb*ASN*-silenced plants were far less susceptible to TRV as they accumulated 60%–90% less viral genomic RNA1 than non-silenced plants agroinoculated with the control TRV-GFP construct (Fig. 5D). Reduction of TRV levels occurred only in Nb*ASN*-silenced plants, but not in Nb*NRIP1*- or Nb*DIN11*-silenced plants, which supports the conclusion that low TRV accumulation is caused by knockdown of Nb*ASN*.

Given that Nb*ASN* was inducible by PVX in *N. benthamiana* (Fig. 4), we wondered whether silencing of Nb*ASN* could also interfere with PVX accumulation in this species. To explore this

idea, we adopted a PVX-based silencing strategy to challenge *N. benthamiana* plants with an infectious PVX construct containing a fragment of Nb*ASN*. qRT-PCR analysis showed that the endogenous Nb*ASN* transcript levels were diminished by about 35% in systemically infected leaves relative to those observed in plants infected with a PVX-GFP vector (Fig. 5E). Remarkably, partial silencing of Nb*ASN* transcripts was sufficient to cause a significant reduction (80%) in PVX RNA levels in the upper infected leaves (Fig. 5E). In these plants, upper silenced leaves infected with PVX-NbASN did not exhibit a distinguishable phenotype with respect to the non-silenced leaves infected with PVX-GFP (data not shown), perhaps because suppression of the endogenous Nb*ASN* gene was incomplete in PVX-NbASN-infected plants.

Reduced susceptibility to TRV in At*DIN11*- or Nb*ASN*-silenced plants is not caused by a general activation of defence genes

Our findings that virus accumulation was drastically impaired in Arabidopsis plants in which *DIN11* transcripts were silenced or in *N. benthamiana* leaves with reduced Nb*ASN* transcript levels prompted us to investigate whether the inactivation of *DIN11* or Nb*ASN* stimulated an antiviral plant defence response. To test this possibility, we first conducted expression analyses of *Pathogenesis-related 1* (At*PR1*, At2g14610) and *Plant defensin 1.2* (At*PDF1.2*, At5g44420) genes in the hairpin *DIN11* RNAi transgenic L10 and L21 lines. *PR1* and *PDF1.2* are commonly used to monitor SA- and jasmonic acid (JA)-dependent defence responses (Loake and Grant, 2007). The SA pathway is typically activated during senescence and virus infections, and resistance to certain RNA viruses is SA dependent (Mayers *et al*., 2005; Whitham *et al*., 2006). Application of MeJA is known to inhibit the replication of several viruses in compatible interactions (Jameson and Clarke, 2002). Interestingly, we found that At*PDF1.2* expression was compromised in both At*DIN11*-silenced RNAi lines compared with Col-0, whereas At*PR1* expression somehow differed between the independent RNAi lines tested (Fig. S3, see Supporting Information). qRT-PCR using RNA preparations from TRV-infected plants revealed that At*PR1* and At*PDF1.2* transcripts accumulated to comparable levels to those found in non-infected plants. This finding suggests that lower TRV levels in our *DIN11* RNAi lines were not caused by the elevated expression of these two defence markers (Fig. 6A).

To determine whether silencing of *NbASN* in *N. benthamiana* plants infected with TRV-NbASN correlated with the activation of defensive genes, the expression of Nb*PR1* (G1FNL9) and *Heat-shock protein 70* (Nb*HSP70*, GQ354819.1) was examined using the same RNA samples as employed for Nb*ASN* and TRV accumulation in transient expression assays. We chose to test Nb*HSP70* expression because HSPs are associated with plant virus replication (Aranda *et al*., 1996; Mine *et al*., 2012). qRT-PCR revealed that Nb*PR1* and Nb*HSP70* transcript levels were reduced by nearly 70%–80% in NbASN-silenced leaves infected with TRV-NbASN compared with non-silenced, TRV-GFP-infected controls (Fig. 6B).

We next investigated the expression pattern of Nb*PR1* and Nb*HSP70* in TRV-infected leaves in which a 35S-driven construct containing the Arabidopsis At*DIN6* homologue gene had been agroinjected 2 days prior to virus inoculation. Transient accumulation of At*DIN6* transcripts was corroborated by qRT-PCR compared with control plants infiltrated with an empty vector (Fig. 6C). We found that TRV levels in leaves expressing At*DIN6* were similar to those observed in control leaves infiltrated with an empty vector (Fig. 6C). Both Nb*PR1* and Nb*HSP70* mRNAs accumulated in the presence of *At*DIN6 to the same levels as those observed in control plants infiltrated with empty vector (Fig. 6C). These results suggest that TRV accumulation and induction of Nb*PR1* and Nb*HSP70* are unaffected by the ectopic expression of At*DIN6* (Fig. 6C).

DISCUSSION

In our study, we have shown that TRV induces host gene responses that are similar to those activated during senescence, even though TRV infection occurs in the absence of morphological manifestations of disease. This means that the activation of senescence genes during TRV infection does not necessarily imply the initiation of the senescence syndrome. Collectively, *DIN* genes are activated in leaves undergoing senescence, as well as in leaves subjected to stimuli that normally lead to senescence, such as darkness, phosphate or carbon starvation, wounding or treatment with photosynthesis inhibitors (Fujiki *et al*., 2001). Microarray-based analysis of gene expression indicates that the up-regulation of *DIN* genes also occurs during responses induced by compatible and incompatible fungal and bacterial pathogens, or on treatment with defence-inducing chemical signals (Genevestigator data) (Schenk *et al*., 2005). Therefore, it seems reasonable to anticipate that *DIN* genes are part of the basal metabolic responses used by cells to cope with stresses that may be common to senescence and pathogen infections. However, like many other stress-inducible genes, the function of *DIN* genes remains elusive at this time. In addition, how these genes contribute to the infectious process is an important question that remains unresolved. The main objective of this study was to examine the effect of *DIN1*, *DIN6* and *DIN11* on plant susceptibility to virus infection. We found that At*DIN1*, At*DIN6* and At*DIN11* were broadly regulated in Arabidopsis in response to TRV, whereas transcripts from Nb*NRIP1*, Nb*ASN* and Nb*DIN11* accumulated to significantly increased levels in *N. benthamiana* leaves infected with TRV or PVX. This finding indicates that *DIN* induction probably represents a common response to different viruses in different compatible host species.

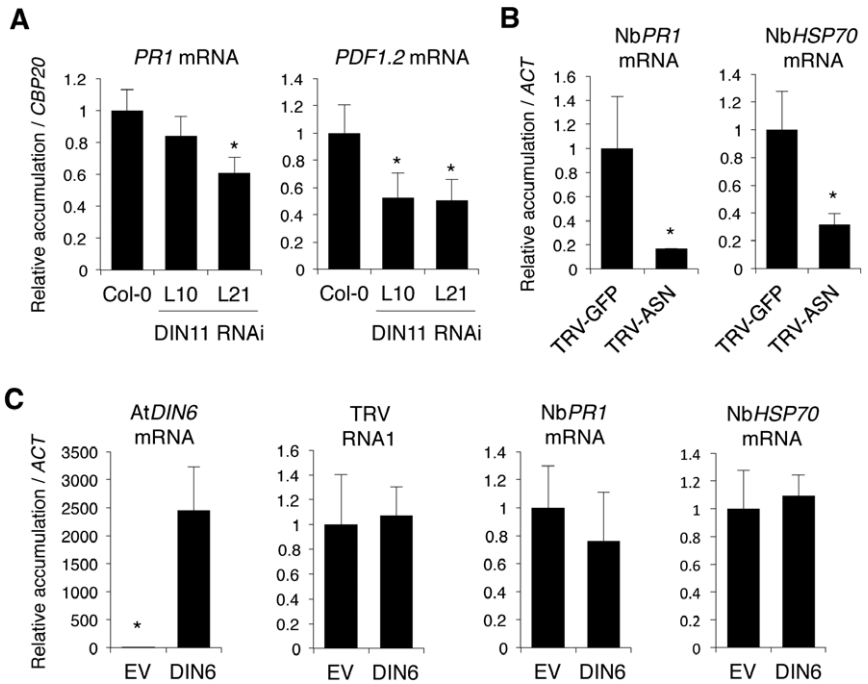

Fig. 6 Effect of At*DIN11* (*Dark-inducible 11*) and *NbASN* (*Asparagine synthetase 1*) on the expression of defence-related genes in *Tobacco rattle virus* (TRV)-infected plants. Expression values, determined by quantitative reverse transcription-polymerase chain reaction (qRT-PCR), are the means of three measurements ± standard deviation (SD). Asterisks indicate statistical significance versus the controls ($P < 0.001$, Duncan's multiple range test). (A) Expression analysis of At*PR1* (*Pathogenesis-related 1*) and At*PDF1.2* (*Plant defensin 1.2*) in upper non-inoculated rosette leaves of Arabidopsis *DIN11* RNA interference (RNAi) lines (L10 and L21) systemically infected with TRV. Values in infected Col-0 plants were assigned a value of unity after At*CBP20* normalization. (B) Expression analysis of Nb*PR1* and Nb*HSP70* (*Heat-shock protein 70*) in upper *N. benthamiana* leaves systemically infected with TRV-NbASN relative to control plants infected with TRV-GFP which were assigned a value of unity after Nb*ACT* normalization. (C) Expression analysis of *NbPR1* and *NbHSP70* in TRV-infected *N. benthamiana* leaves that transiently overexpressed the Arabidopsis At*DIN6* homologue relative to the control leaves in which an empty vector (EV) was agroinoculated (this sample was assigned a value of unity after Nb*ACT* normalization).

Our data indicated that *DIN1* was apparently irrelevant for virus infection in both Arabidopsis and *N. benthamiana*. Similarly, At*DIN1* was shown to be dispensable for disease resistance or tolerance to bacterial and fungal pathogens, although At*DIN1* is strongly elicited during defence responses against these pathogens (Oh *et al*., 1996; Schenk *et al*., 2005). However, *NbNRIP1*, the *N. benthamiana* homologue of At*DIN1*, is required for an effective *N*-mediated defence response to *Tobacco mosaic virus* (TMV) in *N. benthamiana* (Caplan *et al*., 2008). VIGS of Nb*NRIP1* partially abolishes the function of N and allows TMV to spread systemically (Caplan *et al*., 2008). NbNRIP1 mediates the association of the N immune receptor and the TMV-encoded 50-kDa helicase (p50) effector protein to assemble a core recognition complex that allows the plant to detect TMV in infected cells (Caplan *et al*., 2008). Although TRV accumulation was not altered in Nb*NRIP1*-silenced plants, it would be interesting to investigate whether Nb*NRIP1* could also mediate the recognition of putative TRV effector proteins by host immune receptors. The 5'-upstream sequence of the *DIN1* gene contains a TCA motif (TCATCTTCTT) that is highly conserved among genes induced by various stresses (Goldsbrough *et al*., 1993; Oh *et al*., 1996). Therefore, this sequence motif may be involved in the induction of *DIN1* homologues under the stress caused by TRV or PVX in infected cells.

We found that At*DIN6* was not crucial for TRV infection in Arabidopsis. Likewise, At*DIN6* was unnecessary for basal defence and resistance against bacterial and oomycete infection in Arabidopsis (Hwang *et al*., 2011). However, inactivation of the At*DIN6* homologue Nb*ASN* affected negatively TRV and PVX replication in *N. benthamiana*. Interestingly, despite the important role of Nb*ASN* in viral infection in this species, ectopic expression of At*DIN6* had no significant effects on TRV accumulation. A possible explanation is that DIN6/ASN-related functions are not affected by elevated expression of DIN6/ASN-coding genes, as opposed to what is expected from its genetic inactivation. Yet, additional experiments are needed to assess the functionality of the Arabidopsis homologue At*DIN6* in *N. benthamiana*. We demonstrated that VIGS of Nb*ASN* was accompanied by a dramatic reduction in TRV or PVX genomic RNA relative to that in non-silenced control plants. It is worth noting that TRV-mediated

silencing of the target Nb*ASN* transcripts occurs concomitantly with severe morphological defects in the most apical leaves infected with TRV. In contrast, PVX-NbASN-infected plants, in which silencing of Nb*ASN* was only partial, developed normally with an absence of morphological abnormalities. These observations raise the question of whether symptoms are uniquely caused by disruption of Nb*ASN* functions or are also influenced by specific host–virus interactions. Interestingly, VIGS of the *DIN6* homologue gene of *Capsicum annuum* (Ca*AS1*) was found to interfere with pathogen susceptibility by enhancing bacterial infections in pepper (Hwang *et al*., 2011). The apparent discrepancies between our observations and those reported by Hwang *et al*. (2011) could be a result of the inherent differences in the experimental approaches and pathogens tested, with different strategies used to infect the plants.

Our results demonstrated that At*DIN11* influences virus susceptibility in Arabidopsis, as manifested by reduced TRV levels in upper non-inoculated leaves of DIN11 RNAi lines at early stages of infection. Furthermore, our results suggested that At*DIN11* supports TRV replication, as the accumulation of viral genomic RNA was partially inhibited in Arabidopsis protoplasts isolated from knockout lines compared with wild-type Col-0. The reduced susceptibility observed in At*DIN11*- and Nb*ASN*-silenced plants cannot be attributed to a boost in the induction of general defence responses during infection, as none of the defence markers tested in this study showed a changed in expression profile in response to viral infection. This observation is remarkable and supports the idea that At*DIN11* and Nb*ASN* have a direct impact on viral susceptibility by modulating virus accumulation upstream and independent of the activation of defence genes. Nevertheless, we cannot exclude the possibility that other components of the defensive reaction respond positively to At*DIN11* or Nb*ASN* levels to dampen virus accumulation. Why TRV and PVX are unable to replicate efficiently when At*DIN11* or Nb*ASN* activity is compromised is unknown.

DIN6 encodes a glutamine-dependent asparagine synthetase that regulates the levels of asparagine in the dark or under carbon-limiting conditions (Lam *et al*., 1994, 1995, 1998). Induction of *DIN6* in virus-infected plants is presumably linked to the deaminating activity of GDH, a component of senescence and plant defence responses that is up-regulated in Arabidopsis infected with TRV (Fernandez-Calvino *et al*., 2014; Pageau *et al*., 2006). Glutamate deamination by GDH releases significant amounts of free ammonium that must be rapidly eliminated to avoid deteriorating effects within the cell (Lam *et al*., 1998; Masclaux-Daubresse *et al*., 2006). Given that asparagine is viewed as an ammonia detoxification product, it is sensible to propose that the activation of *DIN6* could contribute to counteract the toxic effects of excess ammonium produced during the infection and to help maintain cell integrity, thus allowing effective virus multiplication. Gene or functional redundancy could explain, at least in part, why the genetic inactivation of At*DIN6* in the Arabidopsis *din6* mutant has no influence on TRV susceptibility. Indeed, the Arabidopsis genome contains two additional asparagine synthetase homologous genes (At*ASN2* and At*ASN3*), which encode a novel class of asparagine synthetase enzyme with enhanced ammonia-dependent activity (Lam *et al*., 1998). *DIN11* encodes a protein similar to plant dioxygenases that shows a requirement for 2-oxoglutarate as a co-substrate (Fujiki *et al*., 2001; Prescott and John, 1996). Therefore, like *DIN6*, the activation of *DIN11* in TRV-infected plants could be coupled to the GDH-catalysed deamination of glutamate to 2-oxoglutarate (Masclaux-Daubresse *et al*., 2006). However, the precise function of *DIN11* remains largely unknown.

To date, very limited information is available concerning the role of host factors in compatible plant–virus interactions. Our work has identified *DIN6* and *DIN11* as key regulators that support virus infections in systemically infected host plants, and outlines a number of important questions which need to be answered to elucidate the specific mechanisms and molecular pathways involving DIN6 and DIN11 activities during infections in plants.

EXPERIMENTAL PROCEDURES

Plant material, virus inoculation and sampling procedure

All Arabidopsis plants were in the Columbia background (Col-0), and were grown in controlled environment chambers under 16 h/8 h of light/dark at 19–22 °C. Homozygous plants for T-DNA insertion lines *din1* (NASC code N665464, SALK_020571C) and *din6* (NASC code N479505, GK-829B05) were used. Homozygosity of the mutant alleles was verified by PCR genotyping and by sequencing of the PCR products. *din1* contains a T-DNA insertion in the first intron of the At4g35770 locus (genomic location 16 945 146). *din6* contains a T-DNA insertion in the first exon of the At3g47340 gene (genomic location 17 441 009), 35 nucleotides downstream from the translation initiation site. The primers used for PCR genotyping of homozygous mutants are listed in Table S2 (see Supporting Information).

Nicotiana benthamiana plants were grown in controlled environment chambers under 16 h/8 h of light/dark at 25 °C, and were inoculated at approximately 21 days after germination by infiltration of *Agrobacterium tumefaciens* cultures containing TRV PpK20 cDNA clones of RNA1 (pTRV1)- and RNA2 (pTRV2)-derived constructs (mixed in a 1:1 ratio), or containing PVX (pgR107)-recombinant derivatives, as described previously (Liu *et al*., 2002). Three-week-old Arabidopsis plants were inoculated with TRV using extract sap from systemically TRV-infected *N. benthamiana* leaves, as described previously (Donaire *et al*., 2008). Mock inoculation was performed using sap from healthy, non-infected *N. benthamiana* leaves. Virus infection was corroborated by RT-PCR using TRV or PVX sequence-specific primers (Table S3, see Supporting Information).

Unless otherwise indicated, two or three newly emerging leaves per plant were collected from *N. benthamiana* infected with TRV or PVX derivatives used for VIGS at ~16 dai. Two or three upper non-inoculated rosette leaves per plant were collected from mock- and TRV-inoculated Arabidopsis at ~8 dai. Each sample consisted of RNA pooled from four to ten plants.

Construction of TRV- and PVX-derived plasmids

The pTRV1, pTRV2 and pgR107-PVX DNA vectors used in this study have been described previously (Carrington *et al*., 1999; Liu *et al*., 2002). To generate the recombinant TRV-GFP clone, the soluble modified GFP (smGFP) (Chiu *et al*., 1996) gene cassette under the coat protein promoter of *Pea early-browning tobravirus* (PEBV) was inserted into the multiple cloning site (MCS) of pTRV2. To generate the pTRV2 and pgR107 derivatives used for VIGS, cDNA fragments of Nb*NRIP1* (EU332891.1), At*DIN6*/*ASN1* (At3g47340) and Nb*DIN11* transcripts were RT-PCR amplified from RNA preparations and cloned into pCR2.1 vectors (Invitrogen, Barcelona, Spain) for DNA sequencing. A 303-bp fragment of *N. benthamiana* Nb*NRIP1*, which corresponds to nucleotides 58–360, was amplified using NbNRIP1-F and NbNRIP1-R primers. A 306-bp fragment at nucleotide positions 25–330 of Arabidopsis At*DIN6*/*ASN1*, which shares 77% sequence similarity at the nucleotide level with *N. benthamiana* Nb*ASN* (GQ354808/C9DFA8), was amplified using AtDIN6-F and AtDIN6-R primers. A 322-bp fragment, corresponding to nucleotides 462–784 of the *DIN11* homologue of *S. tuberosum* (clone 069B08), was amplified using StDIN11-F and StDIN11-R primers. A 606-bp fragment of the smGFP-protein coding sequence was amplified using GFP-F and GFP-R primers. cDNA fragments were excised from pCR2.1 vectors and inserted into the MCS of TRV2 or pgR107. All primers are listed in Table S3.

Generation of transgenic RNAi lines

The RNAi Gateway® vector pH 7GWIWG2 (II) (Invitrogen) was used to generate an RNAi construct targeted against At*DIN11*. The selected target region comprised a 431-bp fragment from the 5' terminal region of the Arabidopsis At*DIN11* mRNA that was unique to that particular gene. The primers used are listed in Table S4 (see Supporting Information). All constructs were confirmed by DNA sequencing. The resulting plasmid was transformed into *A. tumefaciens* strain GV3101 by electroporation. Arabidopsis plants of the Col-0 ecotype were then transformed using the floral dipping method and selected on the basis of kanamycin resistance (Clough and Bent, 1998). Homozygous T3 transgenic lines were screened for transcript abundance by qRT-PCR, and only transgenic lines containing reduced levels of *DIN11* transcripts relative to the expression in the wild-type were used for virus infection assays.

RNA preparation and real-time qRT-PCR

Details on the minimum information for publication of real-time qPCR experiments are listed in Tables S5 and S6 (see Supporting Information) (Bustin *et al*., 2009). To quantify the absolute copy number of TRV RNA1, a standard curve of known concentration of *in vitro* transcripts was used. Absolute quantification of viral RNA1 was expressed as the number of viral copies per nanogram of total RNA. Sequence-specific primers are listed in Table S7 (see Supporting Information).

Protoplast preparation and transfection

Arabidopsis protoplasts were isolated from rosette leaves of 3-week-old plants and transiently transformed by the polyethylene glycol (PEG) method, as described previously (Yoo *et al*., 2007), using 30 μg of purified pTRV1 plasmid DNA. Transfected protoplasts were cultured for 24 h in a growth chamber under 16 h of light at 20 °C and 8 h of dark at 22 °C. Protoplasts were harvested by centrifugation, suspended in 500 μL of Trizol reagent and stored at −80 °C for total RNA extraction.

Electrolyte leakage detection and chlorophyll quantification

Electrolyte leakage and chlorophyll *a* and *b* levels were measured in inoculated (TRV or mock) and upper non-inoculated leaves as described previously (De Leon *et al*., 2002; Inskeep and Bloom, 1985).

Morphological trait analysis and fitness estimation

Measurements were taken at 16 and 29 dai from at least 30 plants per treatment. The weight and number of total seeds produced from healthy and TRV-infected Arabidopsis plants were measured from at least 30 individual plants per treatment.

Microarray data

CATMAs for gene expression profiling of TRV-infected Arabidopsis were conducted in our group as described previously (Crowe *et al*., 2003; Fernandez-Calvino *et al*., 2014; Rodrigo *et al*., 2012), and deposited at the Gene Expression Omnibus (GEO) under accession numbers GSE15557/155562/15558.

ACKNOWLEDGEMENTS

This work was supported by grants BIO2006-13107 and BIO2009-12004 from the Spanish Ministry of Science and Innovation and Fondo Europeo de Desarrollo Regional (FEDER). IG-B and FJdT were supported by graduate fellowships from MICINN. LF-C was the recipient of a Junta de Ampliación de Estudios (JAE)-Doc contract from Consejo Superior de Investigaciones Científicas (CSIC, Spain). VR-F was the recipient of a Ramon y Cajal contract from the Spanish Ministry of Economy and Competiveness.

The TRV vector was a gift from Dr S. P. Dinesh-Kumar (Yale University, USA). The PVX vector (pgR107) was kindly provided by Dr David C. Baulcombe (University of Cambridge, UK). We thank Ignacio Hamada (Centro de Investigaciones Biológicas-CSIC) for technical assistance.

REFERENCES

Aranda, M.A., Escaler, M., Wang, D. and Maule, A.J. (1996) Induction of HSP70 and polyubiquitin expression associated with plant virus replication. *Proc. Natl. Acad. Sci. USA*, **93**, 15 289–15 293.

Buchanan-Wollaston, V., Earl, S., Harrison, E., Mathas, E., Navabpour, S., Page, T. and Pink, D. (2003) The molecular analysis of leaf senescence—a genomics approach. *Plant Biotechnol. J.* **1**, 3–22.

Buchanan-Wollaston, V., Page, T., Harrison, E., Breeze, E., Lim, P.O., Nam, H.G., Lin, J.F., Wu, S.H., Swidzinski, J., Ishizaki, K. and Leaver, C.J. (2005) Comparative transcriptome analysis reveals significant differences in gene expression and signalling pathways between developmental and dark/starvation-induced senescence in Arabidopsis. *Plant J.* **42**, 567–585.

Bustin, S.A., Benes, V., Garson, J.A., Hellemans, J., Huggett, J., Kubista, M., Mueller, R., Nolan, T., Pfaffl, M.W., Shipley, G.L., Vandesompele, J. and Wittwer, C.T. (2009) The MIQE guidelines: minimum information for publication of quantitative real-time PCR experiments. *Clin. Chem.* **55**, 611–662.

Caplan, J.L., Mamillapalli, P., Burch-Smith, T.M., Czymmek, K. and Dinesh-Kumar, S.P. (2008) Chloroplastic protein NRIP1 mediates innate immune receptor recognition of a viral effector. *Cell*, **132**, 449–462.

Carrington, J.C., Bisseling, T., Collmer, A. and Jones, J.D. (1999) Highlights from the Ninth International Congress on Molecular Plant–Microbe Interactions. *Plant Cell*, **11**, 2063–2069.

Chiu, W., Niwa, Y., Zeng, W., Hirano, T., Kobayashi, H. and Sheen, J. (1996) Engineered GFP as a vital reporter in plants. *Curr. Biol.* **6**, 325–330.

Clough, S.J. and Bent, A.F. (1998) Floral dip: a simplified method for *Agrobacterium*-mediated transformation of *Arabidopsis thaliana*. *Plant J.* **16**, 735–743.

Crowe, M.L., Serizet, C., Thareau, V., Aubourg, S., Rouze, P., Hilson, P., Beynon, J., Weisbeek, P., van Hummelen, P., Reymond, P., Paz-Ares, J., Nietfeld, W. and Trick, M. (2003) CATMA: a complete Arabidopsis GST database. *Nucleic Acids Res.* **31**, 156–158.

De Leon, I.P., Sanz, A., Hamberg, M. and Castresana, C. (2002) Involvement of the Arabidopsis alpha-DOX1 fatty acid dioxygenase in protection against oxidative stress and cell death. *Plant J.* **29**, 61–62.

Donaire, L., Barajas, D., Martinez-Garcia, B., Martinez-Priego, L., Pagan, I. and Llave, C. (2008) Structural and genetic requirements for the biogenesis of tobacco rattle virus-derived small interfering RNAs. *J. Virol.* **82**, 5167–5177.

Espinoza, C., Medina, C., Somerville, S. and Arce-Johnson, P. (2007) Senescence-associated genes induced during compatible viral interactions with grapevine and Arabidopsis. *J. Exp. Bot.* **58**, 3197–3212.

Fernandez-Calvino, L., Osorio, S., Hernandez, M.L., Hamada, I.B., Del Toro, F.J., Donaire, L., Yu, A., Bustos, R., Fernie, A.R., Martínez-Rivas, J.M. and Llave, C. (2014) Virus-induced alterations in primary metabolism modulate susceptibility to tobacco rattle virus in Arabidopsis. *Plant Physiol.* **166**, 1821–1838.

Fujiki, Y., Yoshikawa, Y., Sato, T., Inada, N., Ito, M., Nishida, I. and Watanabe, A. (2001) Dark-inducible genes from *Arabidopsis thaliana* are associated with leaf senescence and repressed by sugars. *Physiol. Plant.* **111**, 345–352.

Fujiki, Y., Nakagawa, Y., Furumoto, T., Yoshida, S., Biswal, B., Ito, M., Watanabe, A. and Nishida, I. (2005) Response to darkness of late-responsive dark-inducible genes is positively regulated by leaf age and negatively regulated by calmodulin-antagonist-sensitive signalling in *Arabidopsis thaliana*. *Plant Cell Physiol.* **46**, 1741–1746.

Gan, S. and Amasino, R.M. (1997) Making sense of senescence (molecular genetic regulation and manipulation of leaf senescence). *Plant Physiol.* **113**, 313–319.

Gepstein, S., Sabehi, G., Carp, M.J., Hajouj, T., Nesher, M.F., Yariv, I., Dor, C. and Bassani, M. (2003) Large-scale identification of leaf senescence-associated genes. *Plant J.* **36**, 629–642.

Goldsbrough, A.P., Albrecht, H. and Stratford, R. (1993) Salicylic acid-inducible binding of a tobacco nuclear protein to a 10 bp sequence which is highly conserved amongst stress-inducible genes. *Plant J.* **3**, 563–571.

Herbers, K., Takahata, Y., Melzer, M., Mock, H.P., Hajirezaei, M. and Sonnewald, U. (2000) Regulation of carbohydrate partitioning during the interaction of *Potato virus Y* with tobacco. *Mol. Plant Pathol.* **1**, 51–59.

Hwang, I.S., An, S.H. and Hwang, B.K. (2011) Pepper asparagine synthetase 1 (CaAS1) is required for plant nitrogen assimilation and defense responses to microbial pathogens. *Plant J.* **67**, 749–762.

Inskeep, W.P. and Bloom, P.R. (1985) Extinction coefficients of chlorophyll a and b in N,N-dimethylformamide and 80% acetone. *Plant Physiol.* **77**, 483–485.

Jameson, P. and Clarke, S. (2002) Hormone–virus interaction in plants. *Crit. Rev. Plant Sci.* **21**, 205–228.

Lam, H.M., Peng, S.S. and Coruzzi, G.M. (1994) Metabolic regulation of the gene encoding glutamine-dependent asparagine synthetase in *Arabidopsis thaliana*. *Plant Physiol.* **106**, 1347–1357.

Lam, H.M., Coschigano, K., Schultz, C., Melo-Oliveira, R., Tjaden, G., Oliveira, I., Ngai, N., Hsieh, M.H. and Coruzzi, G. (1995) Use of Arabidopsis mutants and genes to study amide amino acid biosynthesis. *Plant Cell*, **7**, 887–898.

Lam, H.M., Hsieh, M.H. and Coruzzi, G. (1998) Reciprocal regulation of distinct asparagine synthetase genes by light and metabolites in *Arabidopsis thaliana*. *Plant J.* **16**, 345–353.

Lim, P.O. and Nam, H.G. (2005) The molecular and genetic control of leaf senescence and longevity in Arabidopsis. *Curr. Top. Dev. Biol.* **67**, 49–83.

Lin, J.F. and Wu, S.H. (2004) Molecular events in senescing Arabidopsis leaves. *Plant J.* **39**, 612–628.

Lin, S.S., Wu, H.W., Elena, S.F., Chen, K.C., Niu, Q.W., Yeh, S.D., Chen, C.C. and Chua, N.H. (2009) Molecular evolution of a viral non-coding sequence under the selective pressure of amiRNA-mediated silencing. *PLoS Pathog.* **5**, e100031.

Liu, Y., Schiff, M., Marathe, R. and Dinesh-Kumar, S.P. (2002) Tobacco Rar1, EDS1 and NPR1/NIM1 like genes are required for N-mediated resistance to tobacco mosaic virus. *Plant J.* **30**, 415–429.

Loake, G. and Grant, M. (2007) Salicylic acid in plant defence—the players and protagonists. *Curr. Opin. Plant Biol.* **10**, 466–472.

van Loon, L.C., Rep, M. and Pieterse, C.M. (2006) Significance of inducible defense-related proteins in infected plants. *Annu. Rev. Phytopathol.* **44**, 135–162.

Love, A.J., Yun, B.W., Laval, V., Loake, G.J. and Milner, J.J. (2005) Cauliflower mosaic virus, a compatible pathogen of Arabidopsis, engages three distinct defense-signaling pathways and activates rapid systemic generation of reactive oxygen species. *Plant Physiol.* **139**, 935–948.

Masclaux, C., Valadier, M.H., Brugiere, N., Morot-Gaudry, J.F. and Hirel, B. (2000) Characterization of the sink/source transition in tobacco (*Nicotiana tabacum* L.) shoots in relation to nitrogen management and leaf senescence. *Planta*, **211**, 510–518.

Masclaux-Daubresse, C., Reisdorf-Cren, M., Pageau, K., Lelandais, M., Grandjean, O., Kronenberger, J., Valadier, M.H., Feraud, M., Jouglet, T. and Suzuki, A. (2006) Glutamine synthetase–glutamate synthase pathway and glutamate dehydrogenase play distinct roles in the sink–source nitrogen cycle in tobacco. *Plant Physiol.* **140**, 444–456.

Mayers, C.N., Lee, K.C., Moore, C.A., Wong, S.M. and Carr, J.P. (2005) Salicylic acid-induced resistance to Cucumber mosaic virus in squash and *Arabidopsis thaliana*: contrasting mechanisms of induction and antiviral action. *Mol. Plant–Microbe Interact.* **18**, 428–434.

Mine, A., Hyodo, K., Tajima, Y., Kusumanegara, K., Taniguchi, T., Kaido, M., Mise, K., Taniguchi, H. and Okuno, T. (2012) Differential roles of hsp70 and hsp90 in the assembly of the replicase complex of a positive-strand RNA plant virus. *J. Virol.* **86**, 12 091–12 104.

Oh, S.A., Lee, S.Y., Chung, I.K., Lee, C.H. and Nam, H.G. (1996) A senescence-associated gene of *Arabidopsis thaliana* is distinctively regulated during natural and artificially induced leaf senescence. *Plant Mol. Biol.* **30**, 739–754.

Pageau, K., Reisdorf-Cren, M., Morot-Gaudry, J.F. and Masclaux-Daubresse, C. (2006) The two senescence-related markers, GS1 (cytosolic glutamine synthetase) and GDH (glutamate dehydrogenase), involved in nitrogen mobilization, are differentially regulated during pathogen attack and by stress hormones and reactive oxygen species in *Nicotiana tabacum* L. leaves. *J. Exp. Bot.* **57**, 547–557.

Pontier, D., Gan, S., Amasino, R.M., Roby, D. and Lam, E. (1999) Markers for hypersensitive response and senescence show distinct patterns of expression. *Plant Mol. Biol.* **39**, 1243–1255.

Prescott, A.G. and John, P. (1996) DIOXYGENASES: molecular structure and role in plant metabolism. *Annu. Rev. Plant Physiol. Plant Mol. Biol.* **47**, 245–271.

Quirino, B.F., Normanly, J. and Amasino, R.M. (1999) Diverse range of gene activity during *Arabidopsis thaliana* leaf senescence includes pathogen-independent induction of defense-related genes. *Plant Mol. Biol.* **40**, 267–278.

Quirino, B.F., Noh, Y.S., Himelblau, E. and Amasino, R.M. (2000) Molecular aspects of leaf senescence. *Trends Plant Sci.* **5**, 278–282.

Rodrigo, G., Carrera, J., Ruiz-Ferrer, V., del Toro, F.J., Llave, C., Voinnet, O. and Elena, S.F. (2012) A meta-analysis reveals the commonalities and differences in *Arabidopsis thaliana* response to different viral pathogens. *PLoS ONE*, **7**, e40526.

Schenk, P.M., Kazan, K., Rusu, A.G., Manners, J.M. and Maclean, D.J. (2005) The SEN1 gene of Arabidopsis is regulated by signals that link plant defence responses and senescence. *Plant Physiol. Biochem.* **43**, 997–1005.

Schippers, J.H., Nunes-Nesi, A., Apetrei, R., Hille, J., Fernie, A.R. and Dijkwel, P.P. (2008) The Arabidopsis onset of leaf death5 mutation of quinolinate synthase affects nicotinamide adenine dinucleotide biosynthesis and causes early ageing. *Plant Cell*, **20**, 2909–2925.

Shalitin, D. and Wolf, S. (2000) Cucumber mosaic virus infection affects sugar transport in melon plants. *Plant Physiol.* **123**, 597–604.

Torres, M.A. and Dangl, J.L. (2005) Functions of the respiratory burst oxidase in biotic interactions, abiotic stress and development. *Curr. Opin. Plant Biol.* **8**, 397–403.

Weaver, L.M., Gan, S., Quirino, B. and Amasino, R.M. (1998) A comparison of the expression patterns of several senescence-associated genes in response to stress and hormone treatment. *Plant Mol. Biol.* **37**, 455–469.

Whitham, S.A., Quan, S., Chang, H.S., Cooper, B., Estes, B., Zhu, T., Wang, X. and Hou, Y.M. (2003) Diverse RNA viruses elicit the expression of common sets of genes in susceptible *Arabidopsis thaliana* plants. *Plant J.* **33**, 271–283.

Whitham, S.A., Yang, C. and Goodin, M.M. (2006) Global impact: elucidating plant responses to viral infection. *Mol. Plant–Microbe Interact.* **19**, 1207–1215.

Wise, R.P., Moscou, M.J., Bogdanove, A.J. and Whitham, S.A. (2007) Transcript profiling in host–pathogen interactions. *Annu. Rev. Phytopathol.* **45**, 329–369.

Yoo, S.D., Cho, Y.H. and Sheen, J. (2007) Arabidopsis mesophyll protoplasts: a versatile cell system for transient gene expression analysis. *Nat. Protoc.* **2**, 1565–1572.

Zimmermann, P., Hirsch-Hoffmann, M., Hennig, L. and Gruissem, W. (2004) GENEVESTIGATOR. Arabidopsis microarray database and analysis toolbox. *Plant Physiol.* **136**, 2621–2632.

SUPPORTING INFORMATION

Additional Supporting Information may be found in the online version of this article at the publisher's website:

Fig. S1 Analysis of senescence-associated traits during late *Tobacco rattle virus* (TRV) infection in Arabidopsis.

Fig. S2 Transcript accumulation of *Dark-inducible* (*DIN*) genes in response to *Tobacco rattle virus* (TRV) infection in Arabidopsis.

Fig. S3 Expression of defence-related genes in non-infected *DIN11* RNA interference (RNAi) lines.

Table S1 List of genes showing similar responsiveness to *Tobacco rattle virus* (TRV) infection, dark-induced senescence and age-dependent senescence.

Table S2 List of primers used for polymerase chain reaction (PCR) genotyping.

Table S3 List of primers used for virus amplification and in the construction of *Tobacco rattle virus* (TRV)-based virus-induced gene silencing (VIGS) vectors.

Table S4 List of primers used in the construction of *Dark-inducible* (*DIN*)-overexpressing Arabidopsis transgenic lines.

Table S5 Minimum information required for publication of quantitative real-time reverse transcription-polymerase chain reaction (RT-PCR) experiments involving messenger RNAs.

Table S6 Minimum information required for publication of quantitative real-time reverse transcription-polymerase chain reaction (RT-PCR) experiments involving absolute quantification of viral RNA.

Table S7 List of primers used in quantitative real-time reverse transcription-polymerase chain reaction (RT-PCR).